THE JOURNAL OF PHYSICAL CHEMISTRY B

Article

pubs.acs.org/JPCB

Importance of Boundary on the Electrophoresis of a Soft Cylindrical Particle

Jyh-Ping Hsu,*[,†,‡] Hong-Ming Lo,[‡] Li-Hsien Yeh,[§] and Shiojenn Tseng*[,⊥]

[†]Department of Chemical Engineering and [‡]Institute of Polymer Science and Engineering, National Taiwan University, Taipei, Taiwan 10617

[§]Department of Chemical and Materials Engineering, National Yunlin University of Science and Technology, Douliou, Yunlin, Taiwan 64002

[⊥]Department of Mathematics, Tamkang University, Tamsui, Taipei, 25137, Taiwan

Supporting Information

ABSTRACT: We modeled the electrophoresis of a soft cylindrical particle comprising a rigid core and a polyelectrolyte layer along the axis of a long, cylindrical pore, and the applicability of the model proposed is verified by the experimental data available in the literature. Previous analysis is extended to the case where the effects of double-layer polarization (DLP) and electroosmotic flow (EOF) can be significant. We show that the interaction between the particle's double layer and the pore, the competition between the effective charge density and the local electric field strength, and the presence of EOF yield interesting and significant results. For example, if EOF is absent, the particle mobility as the bulk salt concentration varies depends highly on the amount of fixed charge of its polyelectrolyte layer: if that amount is small, the mobility decreases monotonically with increasing bulk salt concentration, and if that amount is large, then the mobility shows a local maximum. At a high bulk salt concentration, the longer the particle the larger is its mobility, that trend is reversed if it is low. That local minimum vanishes when the boundary effect is important. If the pore is positively charged, a positively charged particle can be driven to the direction opposite to that of the applied electric field. These provide necessary information for the design of electrophoresis devices.

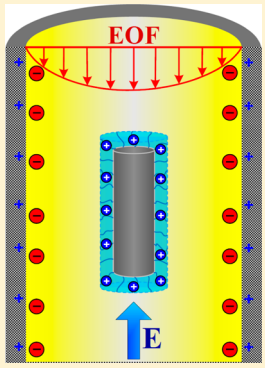

1. INTRODUCTION

Recently, electrophoresis has been applied to small scaled devices such as DNA sequencing,[1] micro- and nanofluidic systems,[2] drug delivery,[3,4] and biosensors.[5] In these cases, both the electric and the hydrodynamic interactions between a particle and the device wall can be significant. For example, in emerging nanofluidic devices used in sensing nanoparticles,[6−9] where the overlapping of the electrical double layer (EDL) of a nanoparticle and that of the device wall is significant under typical conditions, the electrokinetic transport of a nanoparticle is influenced inevitably by the nanofluidic device wall. In addition, because that wall is usually charged, an electroosmotic flow (EOF) is present[10,11] and the nanoparticle behavior is affected accordingly. These imply that a detailed understanding of the boundary effect on the electrophoretic behavior of a nanoparticle is necessary to both elucidating experimental observations and designing sensing devices. Several efforts have been made on that effect. For instance, in a study of the electrophoresis of a rigid finite cylinder of constant surface potential along the axis of an uncharged cylindrical pore, Hsu and Kao[12] concluded that the movement of the former is retarded by the latter. Zhang et al.[13] investigated the electrokinetic translocation of a rigid cylindrical nanoparticle capped with two hemispheres of constant charge density through a nanopore containing a floating electrode. In a study of the electrophoresis of a spherical particle of constant charge density in a tube having a converging−diverging cross section, Qian et al.[14,15] found that the nonuniform boundary establishes a nonuniform electric field, making the electrophoretic behavior of a particle inside different from that inside a uniform boundary.

One of the distinguishing features of recent applications of electrophoresis is that the particles of interest are usually of nonrigid or soft nature. For example, in a study of DNA translocation through a nanopore, Zhang et al.[16] and Yeh et al.[17] proposed a soft, rod-like particle having two hemispherical caps comprising a rigid core and an ion-penetrable layer. They showed that the particle velocity is influenced appreciably by the nanopore. Ohshima was able to derive an analytical expression for the mobility of a spherical soft particle in a salt-free medium.[18] He showed that the electrokinetic behavior of a soft particle is different significantly from that of the corresponding rigid one. Wong et al.[19] studied experimentally the electrophoresis of a microgel with multiple polyelectrolyte layers; the influences of the ionic strength and the molecular weight of polyelectrolyte were discussed. The nonrigid layer of a soft particle is porous and usually contains fixed charge coming from dissociable functional groups. This implies that its presence influences both hydrodynamically and electrically the electrophoretic behavior of the particle and that behavior can

Received: June 4, 2012
Revised: September 18, 2012
Published: September 25, 2012

be different both quantitatively and qualitatively from the behavior of the corresponding rigid particle.

Several attempts have been made on modeling the electrophoresis of a soft particle. For example, assuming low surface potential, Ohshima analyzed the electrophoresis of an isolated soft particle.[20] Because the surface potential is low, the effect of double-layer polarization (DLP) was neglected. This effect was taken into account by Zhang et al.[21] in an analysis of the electrophoresis of a soft particle along the axis of a charged cylindrical pore. Hill et al.[22] numerically studied the electrophoresis of a highly charged polyelectrolyte-coated spherical particle and showed that the presence of polarization and relaxation effects resulting from the charged layer of a particle plays an essential role on its electrophoretic behavior. Allison[23] analyzed the electrophoretic mobility of a dilute suspension of silica sol; both salt concentration and solution pH were taken into account to simulate various experimental conditions. Yeh and Hsu[24] considered the electrophoresis of a spherical polyelectrolyte, an entirely porous particle, in a cylindrical pore. In a study of the electrophoresis of a soft sphere in a spherical cavity Yeh et al.[25] divided soft particles into two categories: type I comprises a rigid, charged core of constant surface potential and an uncharged porous layer; type II comprises a rigid, uncharged core and a porous charged layer. The mobility of a type I particle increases with decreasing double-layer thickness, which is qualitatively similar to that of a rigid particle,[26] but the mobility of a type II particle decreases with decreasing double-layer thickness.[27] Duval and Ohshima[28] analyzed the electrophoresis of diffuse soft particles with inhomogeneous distribution of charge density in polymer gel layer; however, they focused on an isolated spherical particle, and the EOF arising from the charge boundary as well as the particle−boundary interactions were not considered.

A simplification usually made in electrophoresis analysis is assuming a spherical particle. Although this makes mathematical analysis simpler, it can be unrealistic for particles such as DNAs or micelles under specific conditions, where assuming a finite cylinder is more adequate.[29,30] Assuming low surface potential and thin electric double layer, Wang and Keh[31] modeled the electrophoresis of a long, rigid cylinder in a planner slit. Ye et al.[32] considered a cylinder of constant surface potential for the case of very thin electric double layer. Ohshima analyzed the electrophoresis of a long, cylindrical particle having a rigid, charged core and an uncharged porous layer under the conditions of low surface potential.[33] Under the conditions of weak applied electric field, low surface potential, and arbitrary double-layer thickness, Yeh et al.[34] studied the electrophoresis of a membrane-coated cylindrical particle positioned eccentrically along the axis of a narrow cylindrical pore. Ren and Li[35] and Liu et al.[36] investigated the influence of electroosmotic flow (EOF) on the electrophoretic behavior of a rigid cylindrical particle in a microchannel and in a long cylindrical tube, respectively. In a study of DNA translocation, simulated by a cylindrical particle moved in a nanotube, Ai et al.[37] concluded that EOF is important. A general boundary element methodology was developed by Allison et al.[38] to study the electrophoretic behavior of soft colloidal particles of arbitrary size, shape, charge, and polyelectrolyte layer geometry, taking into account the boundary effect. The above studies reveal that both the porous layer of a particle and its geometry can influence significantly its electrophoretic behavior.

Considering the fast growth in relevant applications, we investigate the electrophoresis of a finite, soft cylindrical particle in a long cylindrical pore. The soft particle comprises a rigid core and a polyelectrolyte layer, simulating, for example, clay, protein, and DNA. Note that the particle in the present geometry experiences a much more significant boundary effect than those considered in the literature, such as a sphere in a spherical cavity,[39] a sphere in a cylindrical pore,[40−44] and an ellipsoid in a cylindrical pore.[45,46] Because the effect of both double-layer polarization (DLP) and EOF are considered, the present model is more general and realistic than most of the previous ones. To examine the influences of the bulk salt concentration, the ratio of pore radius/particle radius, the particle aspect ratio, the strength of EOF, and the fixed charge density of the particle on its electrophoretic behavior, a detailed numerical simulation is conducted. The results gathered provide necessary information for the design of electrophoresis devices.

2. THEORETICAL MODEL

Let us consider the electrophoresis of a soft cylindrical particle of radius a and length $2d$ covered by a polyelectrolyte layer of thickness c along the axis of a long, cylindrical pore of radius b. In Figure 1, r and z are the radial and axial distances,

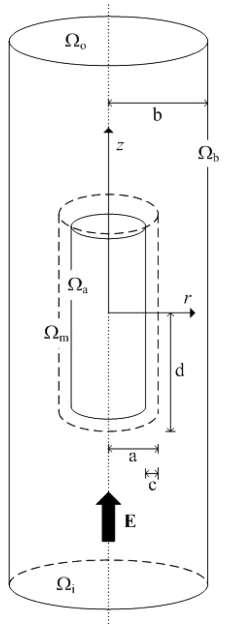

Figure 1. Electrophoresis of a soft cylinder of radius a and half-length d with a polyelectrolyte layer of thickness c along the axis of a long cylindrical pore of radius b subject to an applied electric field **E** in the z direction; r and z are the radial and axial distances, respectively, of cylindrical coordinates adopted with the origin at the center of the pore. Ω_a, Ω_m, and Ω_b are the surface of the particle's rigid core, the fluid−membrane interface, and the pore surface, respectively. For convenience, we define a computation domain with boundaries Ω_b, Ω_i, and Ω_o.

respectively, of a cylindrical coordinates chosen with the origin at the center of the particle and **E** is an applied uniform electric field of strength E in the z direction. The pore contains an aqueous z_1:z_2 electrolyte solution, where z_1 and z_2 are the valences of cations and anions, respectively. Let Ω_a, Ω_m, and Ω_b be the surface of the particle's rigid core, the fluid−membrane interface, and the pore surface, respectively. For convenience,

we define a computation domain with boundaries Ω_b, Ω_i, and Ω_o.

Suppose that the system is at a pseudo-steady state and the liquid is an incompressible Newtonian fluid of constant physical properties. Let ϕ and $\mathbf{u}$ be the electrical potential and liquid velocity, respectively, ε, ρ, ρ_{fix}, e, k_B, T, η, γ, and p be the liquid permittivity, space charge density of mobile ions, fixed charge density in the polyelectrolyte layer, elementary charge, Boltzmann constant, absolute temperature, liquid viscosity, and pressure, respectively, and D_j, n_j, and z_j be the diffusivity, number concentration, hydrodynamic frictional coefficient per unit volume of the polyelectrolyte layer, and valence of ionic species j, respectively. Then the present problem can be described by the set of equations below[16,20,47]

$$\nabla^2\phi = -\frac{\rho + i\rho_{fix}}{\varepsilon} = -\sum_{j=1}^{2}\frac{z_j e n_j}{\varepsilon} - i\frac{\rho_{fix}}{\varepsilon} \quad (1)$$

$$\nabla\cdot\mathbf{u} = 0 \quad (2)$$

$$\nabla p + \eta\nabla^2\mathbf{u} - \rho\nabla\phi - i\gamma\mathbf{u} = \mathbf{0} \quad (3)$$

$$\nabla\cdot\left[-D_j\left(\nabla n_j + \frac{z_j e}{k_B T} n_j \nabla\phi\right) + n_j\mathbf{u}\right] = 0 \quad (4)$$

Here $i = 1$ for the polyelectrolyte layer and $i = 0$ for the region outside it.

Under the conditions of weak applied electric field, i.e., $E < 25$ kV m^{-1}, a perturbation approach is applicable,[48] where the original problem is partitioned into an equilibrium problem and a perturbed problem, taking account of the effect of double-layer polarization. The transformed governing equations are given in the Supporting Information.

We assume the following. (i) Both the surface of the particle's rigid core and that of the pore remain at a constant surface charge density, nonconductive, impermeable to ionic species, and nonslip. (ii) Both the fluid and the electric fields far away from the particle (on Ω_i and Ω_o) are uninfluenced by its presence.[34] Under typical conditions, the end effect of a cylindrical pore can be neglected if its length exceeds ca. 10 times that of a cylindrical particle.[34] (iii) Both the permittivity and the viscosity of the liquid inside the polyelectrolyte layer are the same as those outside it. Therefore, the electrical potential, electric field, liquid velocity, normal stress, and tangential stress are all continuous on the polyelectrolyte–liquid interface.[34,49]

Because the boundary conditions for the flow field involve an unknown particle velocity, a trial-and-error procedure is required. This difficulty can be avoided by adopting the procedure proposed by O'Brien and White.[48] Here, the original problem is partitioned into two subproblems: the particle moves with a constant velocity U in the absence of $\mathbf{E}$ in the first subproblem, and $\mathbf{E}$ is applied but is held fixed in the second subproblem. If the applied electric field $\mathbf{E}$ is much weaker than that established by the particle and the pore, then each dependent variable can be partitioned approximately into an equilibrium component, the value of that variable when $\mathbf{E}$ is absent, and a perturbed component contributed by $\mathbf{E}$. Details about this procedure are given in the Supporting Information. Assuming a pseudo-steady state condition, the mobility of the particle, $\mu = U/E$, can be evaluated based on a force balance stated in the Supporting Information. For convenience, we define the scaled electrophoretic mobility of a particle, μ^*, as

$$\mu^* = \frac{U^*}{E^*} \quad (5)$$

Here, $U^* = U/[\varepsilon(k_B T/e)^2/\eta a]$ and $E^* = E/[k_B T/ea]$ are the scaled electrophoretic mobility of the particle and the scaled strength of $\mathbf{E}$, respectively.

3. RESULTS AND DISCUSSION

FlexPDE (version 4.24, PDE Solutions, Spokane Valley, WA) is adopted to solve the present boundary value problem. To verify its applicability, the electrophoresis of an isolated soft spherical particle comprising a hard core of low, constant surface potential and an uncharged membrane layer solved analytically by Ohshima[20] is resolved by the present approach. The results obtained are illustrated in the Supporting Information, and as can be seen, the present approach is able to reproduce accurately the analytical result of Ohshima.[20]

In the present problem, the electrophoretic behavior of a particle can be influenced by the EDL thickness (or bulk electrolyte concentration), size of the pore, particle aspect ratio, fixed charged density of the particle's polyelectrolyte layer, and pore's surface charge density. We perform a detailed numerical simulation to examine the influences of these parameters. For convenience, the particle radius a is fixed, and we define $\lambda^{-1} = (\eta/\gamma)^{1/2}$, the softness parameter of the polyelectrolyte layer or a shielding length characterizing the extent of flow penetration into that layer.[17,49,50] Typically, λ^{-1} ranges from 0.1 to 10 nm.[34,51,52] For illustration, we assume $\lambda a = 5$ and $c/a = 0.2$. In addition, we consider an aqueous KCl solution at $T = 298$ K, yielding $z_1 = -z_2 = 1$ and $Pe_1 = Pe_2 = 0.235$.[53] We assume that the particle's rigid core is uncharged ($\sigma_a^* = 0$) for simplicity.

3.1. Influences of EDL Thickness and Fixed Charge Density. Figure 2 shows the influences of the EDL thickness

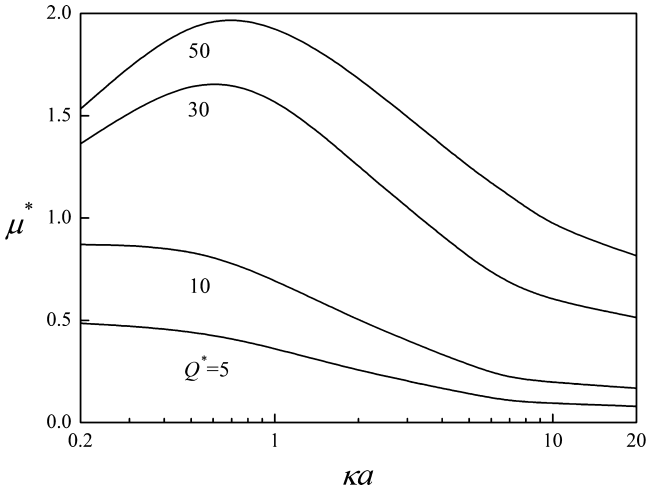

Figure 2. Variations of the scaled mobility μ^* as a function of κa for various values of Q^* at $b/a = 5$, $d/a = 1$, and $\sigma_b^* = 0$.

measured by κa and the polyelectrolyte layer's fixed charge density measured by $Q^* = \rho_{fix}/(\varepsilon k_B T/ea^2)$ on the scaled mobility μ^*. For simplicity, we assume that the pore surface is free of fixed charge in the present case. Because the particle radius a is fixed, the variation of κa comes from that of the bulk electrolyte concentration. It is interesting to note in Figure 2 that the qualitative behavior of μ^* as κa varies depends highly on Q^*. For small Q^*, μ^* decreases monotonically with increasing κa. This is consistent with the typical electrophoretic

dx.doi.org/10.1021/jp305473s | J. Phys. Chem. B 2012, 116, 12626–12632

behavior of soft nanoparticles[54] and observed experimentally in a study of the electrokinetic translocation of single dsDNA, which can be viewed as a cylindrical nanoparticle,[55] through a solid-state nanopore.[56] However, as Q^* gets large, μ^* shows a local maximum at $\kappa a \cong 0.7$. These can be explained by the behavior of the effective charge density $|\rho + \rho_{fix}|$ and the local electric field strength. In the case of small Q^*, if κa is small, because the particle's polyelectrolyte layer is enclosed by EDL, counterions are not confined inside the layer. As κa increases, so is the amount of counterions inside the polyelectrolyte layer and $|\rho + \rho_{fix}|$ deceases accordingly. In the case of large Q^*, in addition to the effect of $|\rho + \rho_{fix}|$, that of the local electric field also plays a role. Table 1 shows the variations in the averaged

Table 1. Variations of the Averaged Scaled Local Electric Field Strength, $E^*_{local} \times 10^4$, As a Function of κa at Two Levels of the Scaled Fixed Charged Density Q^* for the Case where $b/a = 5$, $d/a = 1$, and $\sigma^*_b = 0$

	κa				
Q^*	0.2	1	3	5	7
5	5.03	5.13	5.15	5.25	4.71
30	2.44	3.44	4.53	4.94	5.06

scaled local electric field strength, $E^*_{local} = \int -(\partial\delta\phi^*/\partial z)d\Omega^*_m / \int d\Omega^*_m$, as a function of κa at two levels of Q^*. Here, $\delta\phi^* = \delta\phi/(k_BT/e)$ is the scaled value of $\delta\phi$, the perturbed potential arising the application of $\mathbf{E}$, and $\Omega^*_m = \Omega_m/a^2$ is the scaled Ω_m. As can be seen in Table 1, E^*_{local} increases with increasing κa at $Q^* = 30$ but remains roughly the same as $Q^* = 5$. The presence of the local maximum in μ^* is the result of competition between the increase of E^*_{local} and that of counterions inside the polyelectrolyte layer. As seen in Figure S2 of the Supporting Information, μ^* is dominated by the electrical driving force coming from $\mathbf{E}$ but not the hydrodynamic drag due to the flow of liquid and EOF. This is consistent with the observation of Yeh et al.[25] in the electrophoresis of an ion-penetrable sphere in a spherical cavity.

Figure 2 also reveals that as κa gets large (i.e., the salt concentration gets high), μ^* approaches a finite, nonzero constant value, which is typical of the soft colloidal particles.[49,51,57] However, this behavior is inconsistent with the behavior of rigid particles (i.e., in the absence of the polyelectrolyte layer) with constant surface charge density,[58] where the mobility vanishes at infinitely high salt concentration (i.e., $\kappa a \to \infty$). This is because if κa is sufficiently large, the soft particle is significantly screened by counterions, resulting in a saturated fixed charge density (or effective charge density)[59] and a concentration-independent electrophoretic velocity. A similar phenomenon was found in a study of the electrokinetic DNA translocation through a solid-state nanopore,[56] where the translocation time reached a saturated value when the salt concentration is sufficiently high.

3.2. Influence of Particle Aspect Ratio. Figure 3 summarizes the influences of the particle aspect ratio (d/a) on its scaled mobility, μ^*. This figure reveals that for all the levels of d/a examined, μ^* shows a local maximum as the thickness of EDL κa varies. Note that if κa is large (thin EDL), the larger the d/a the larger the μ^*; however, that trend is reversed when κa is small. For a medium large κa, there is no general relationship between μ^* and d/a. The decrease in μ^* with increasing d/a at small κa is unexpected. This arises mainly from the competition between the electric driving force and the

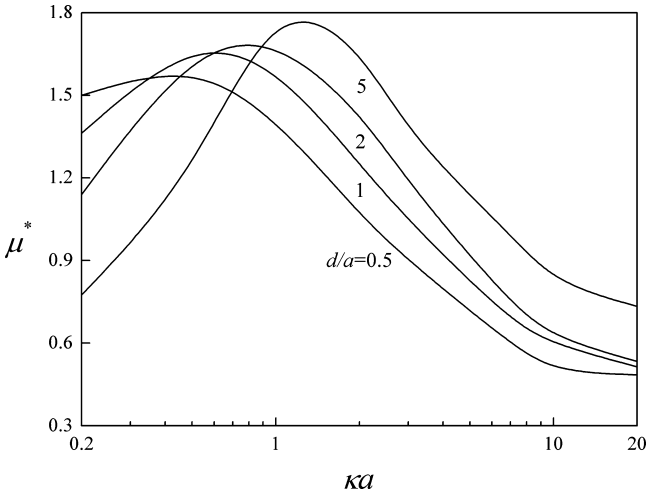

Figure 3. Variations of the scaled mobility μ^* as a function of κa at various values of d/a at $Q^* = 30$, $b/a = 5$, and $\sigma^*_b = 0$.

hydrodynamic drag acting on the particle. Because the particle radius a is fixed, the larger the d/a the longer the particle, the greater the amount of surface charge, and, therefore, the greater the electric driving force acting on the particle. However, the hydrodynamic drag acting on the particle also increases with increasing d/a. If κa is small, the hydrodynamic drag dominates and μ^* decreases with increasing d/a. On the other hand, if it is large, the electric driving force dominates and μ^* is increasing with increasing d/a. Details about the behavior of the forces acting on the particle are summarized in Figure S3 of the Supporting Information.

3.3. Influence of Boundary. The influence of the pore (boundary effect), measured by the ratio of b/a, on the scaled mobility μ^* is illustrated in Figure 4; the larger that ratio the

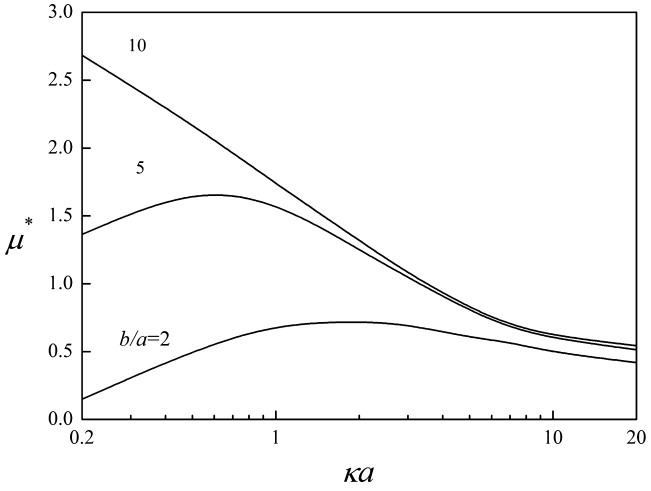

Figure 4. Variations of the scaled mobility μ^* as a function of κa at various values of b/a at $Q^* = 30$, $d/a = 1$, and $\sigma^*_b = 0$.

less significant the boundary effect is. As can be seen in this figure, μ^* increases with increasing b/a, which is expected because the larger the b/a the smaller the hydrodynamic drag acting on the particle coming from the pore. This behavior is consistent with the experimental observation of the electrokinetic translocation of nanoparticles through cylindrical[60] and conical[7] nanopores. It is interesting to note that if b/a is small, μ^* has a local maximum as κa varies but vanishes as b/a gets

dx.doi.org/10.1021/jp305473s | J. Phys. Chem. B 2012, 116, 12626−12632

large. The behavior of μ^* at a large b/a, namely, μ^* decreases monotonically with increasing κa, can be explained by the fact that an increase in the salt concentration yields a reduction in the effective fixed charge of the polyelectrolyte layer, as proposed by Manning.[61] On the other hand, if b/a is small, the interaction between the EDL of the particle and the pore is important so that the behavior of μ^* is similar to those observed in Figures 2 and 3. Note that as $\kappa a \to \infty$, μ^* approaches a constant value, regardless of the value of b/a, which is expected because that interaction is unimportant in this case.

3.4. Influence of a Charged Pore. Let us consider the case where the particle and pore are positively charged. In this case, an EOF is present, which flow in the direction opposite to the applied electric field. Figure 5 presents μ^* as a function of

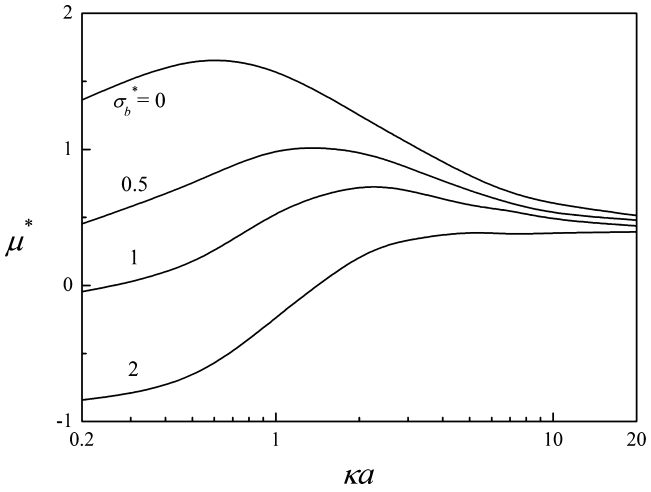

Figure 5. Variations of the scaled mobility μ^* as a function of κa at various values of σ_b^* at $Q^* = 30$, $d/a = 1$, and $b/a = 5$.

κa at various levels of the scaled surface charge density of the pore, σ_b^*. Note that the curve for $\sigma_b^* = 0$ in this figure corresponds to the curve for $Q^* = 30$ in Figure 2. As can be seen in Figure 5, this indicates that μ^* decreases with increasing of σ_b^*, which is expected because the larger σ_b^* the more significant the electroosmotic flow due to the pore. If σ_b^* exceeds a certain level, then the local maximum of μ^* might disappear. In addition, μ^* might change its sign from positive to negative, implying that EOF dominates. It is interesting to see in Figure 5 that if σ_b^* is sufficiently large then as κa increases μ^* changes its sign from negative to positive. This implies that the direction of electrophoresis can be altered by adjusting the bulk electrolyte concentration. These behaviors are consistent with the experimental observation of the electrokinetic translocation of DNA molecules through a rectangular silica nanochannel.[10] If the solution pH is high (e.g., 8), so is the charge density of the nanochannel wall, yielding a significant EOF, and the electrophoretic behavior of DNA molecules is affected significantly. If the salt concentration is high, the electrophoretic behavior of DNA molecules is dominated by EOF (or electrophoresis force). However, if it is sufficiently low, that behavior is dominated by the net effects of EOF and electrophoresis force, implying that the direction of particle velocity can be either positive or negative.[10] Figure 5 also reveals that the significance of EOF decreases with increasing κa, that is, the thinner the EDL the less significant the EOF. This explains that as $\kappa a \to \infty$, μ^* approaches a constant value, regardless of the value of σ_b^*.

The qualitative behavior of μ^* in Figure 6 is similar to that of the curve for $\sigma_b^* = 1$ in Figure 5 and can be explained by the

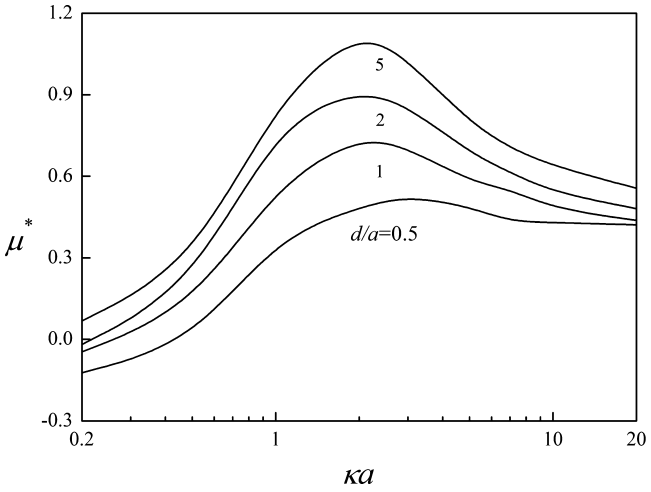

Figure 6. Variations of the scaled mobility μ^* as a function of κa at various values of d/a at $Q^* = 30$, $b/a = 5$, and $\sigma_b^* = 1$.

same reasoning. A comparison between Figures 6 and 3 reveals that the crosses of the curves in the latter vanish in the former, that is, if EOF is significant, μ^* of a longer particle is always larger than that of a shorter one. This is because the presence of EOF has the effect of reducing the importance of the local electric field and EOF dominates when κa is not large.

3.5. Verification of Model by Experimental Data. The applicability of our model is verified by fitting it to the experimental data of Hoagland et al.,[62] where the capillary electrophoresis of high molecular weight duplex DNA, modeled as a soft cylindrical nanoparticle, of radius 1.2 nm in an aqueous NaCl solution was conducted. In this case, $Pe_1(Na^+) = 0.351$, $Pe_2(Cl^-) = 0.23$,[57] and $\sigma_b^* = 0$. To avoid the influence of boundary, a sufficiently large value is assumed for b/a, 10. Figure 7 shows the scaled electrophoretic mobility μ^* as a function of κa. For comparison, the prediction based on Manning's model[61] is also presented. As seen in Figure 7, our result (solid line) agrees very well with the experimental data (discrete symbols). On the other hand, that predicted by Manning fails to describe the general trend of μ^*, especially when κa is small. This is because Manning's model is based on the Debye−Hückel approximation, which is valid only if the electric potential is low, which is not satisfied in the present case. The surface potential of high molecular weight duplex DNA is usually not low, implying that DLP and relaxation effects, both reduce the particle mobility,[24,57] need to be considered. As seen in Figure 7, this also explains why the result based on Manning's model is higher than the experimental data for $\kappa a < 1$.

4. CONCLUSIONS

The electrophoresis analyses in the literature on rigid and soft spherical particles are extended to the case of a soft cylindrical particle comprising a rigid core and a polyelectrolyte layer for the case where the boundary effect can be significant. The geometry considered is capable of simulating, for example, biocolloids such as DNA and particles covered by an artificial membrane layer. The influences of the properties of the

dx.doi.org/10.1021/jp305473s | J. Phys. Chem. B 2012, 116, 12626−12632

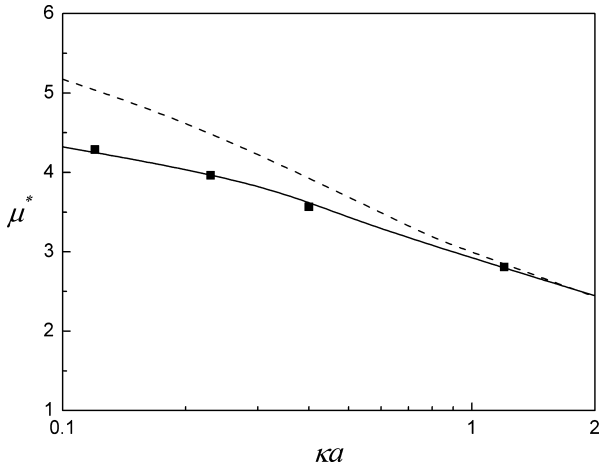

Figure 7. Variations of the scaled mobility μ^* of duplex DNA as a function of κa for the case where its radius is 1.2 nm: (discrete symbols) experimental data of Hoagland et al.;[62] (dashed line) theoretical based on Manning's model;[61] (solid line) present numerical result at $Q^* = 40$, $c/a = 0.38$, $d/a = 0.5$, $\lambda a = 1$, $Pe_1(Na^+) = 0.351$, $Pe_2(Cl^-) = 0.23$, and $\sigma_b^* = 0$.

polyelectrolyte layer, particle aspect ratio, bulk salt concentration, boundary effect, and electroosmotic flow (EOF) on the electrophoretic behavior of the particle are investigated. For an uncharged pore, EOF is absent and we conclude the following. (i) The mobility of a particle as the bulk salt concentration varies depends highly on the amount of fixed charge of its polyelectrolyte layer. If that amount is small, the mobility decreases monotonically with increasing bulk salt concentration. On the other hand, if that amount is large, then the mobility shows a local maximum. These can be explained by the competition between the effective charge density and the local electric field strength. (ii) If the bulk salt concentration is high, the longer the particle the larger is its mobility; however, if it is low, that trend is reversed. No general trend is observed for a medium level of bulk salt concentration. These behaviors arise from the competition between the electric driving force and the hydrodynamic drag acting on the particle. (iii) The more significant the boundary effect the greater the hydrodynamic drag acting on the particle and, therefore, the smaller the mobility. If the boundary effect is not that appreciable, the mobility has a local minimum as the bulk salt concentration varies, but this local minimum vanishes as that effect becomes important. The former is due to a reduction in the effective fixed charge of the polyelectrolyte layer; the latter arises from the interaction between the double layer of the particle and the pore. If the pore is positively charged, we conclude the following. (i) EOF is present with its direction opposite to that of the applied electric field, thereby reducing the mobility of a positively charged particle. (ii) The lower the bulk salt concentration the more significant the influence of EOF, and if the pore's surface charge density is sufficiently high, a positively charged particle can be driven to the direction opposite to that of the applied electric field.

■ ASSOCIATED CONTENT

Ⓢ Supporting Information

(i) Summary of the perturbed governing equations and the associate boundary conditions; (ii) details of the solution procedure; (iii) verification of the present code; (iv) forces acting on a particle under various conditions. This material is available free of charge via the Internet at http://pubs.acs.org.

■ AUTHOR INFORMATION

Corresponding Author

*E-mail: jphsu@ntu.edu.tw (J.-P.H.), topology@mail.tku.edu.tw (S.T.).

Notes

The authors declare no competing financial interest.

■ ACKNOWLEDGMENTS

This work was supported by the National Science Council of the Republic of China.

■ REFERENCES

(1) Branton, D.; Deamer, D. W.; Marziali, A.; Bayley, H.; Benner, S. A.; Butler, T.; Di Ventra, M.; Garaj, S.; Hibbs, A.; Huang, X. H.; Jovanovich, S. B.; Krstic, P. S.; Lindsay, S.; Ling, X. S. S.; Mastrangelo, C. H.; Meller, A.; Oliver, J. S.; Pershin, Y. V.; Ramsey, J. M.; Riehn, R.; Soni, G. V.; Tabard-Cossa, V.; Wanunu, M.; Wiggin, M.; Schloss, J. A. *Nat. Biotechnol.* **2008**, *26*, 1146−1153.
(2) Squires, T. M.; Quake, S. R. *Rev. Mod. Phys.* **2005**, *77*, 977−1026.
(3) Hoare, T.; Pelton, R. *Langmuir* **2004**, *20*, 2123−2133.
(4) Lu, Y.; Ballauff, M. *Prog. Polym. Sci.* **2011**, *36*, 767−792.
(5) Nakamura, H.; Karube, I. *Anal. Bioanal. Chem.* **2003**, *377*, 446−468.
(6) Castillo-Fernandez, O.; Salieb-Beugelaar, G. B.; van Nieuwkasteele, J. W.; Bomer, J. G.; Arundell, M.; Samitier, J.; van den Berg, A.; Eijkel, J. C. T. *Electrophoresis* **2011**, *32*, 2402−2409.
(7) Lan, W. J.; Holden, D. A.; Zhang, B.; White, H. S. *Anal. Chem.* **2011**, *83*, 3840−3847.
(8) Lan, W. J.; Holden, D. A.; Liu, J.; White, H. S. *J. Phys. Chem. C* **2011**, *115*, 18445−18452.
(9) Luan, B.; Stolovitzky, G.; Martyna, G. *Nanoscale* **2012**, *4*, 1068−1077.
(10) Stein, D.; Deurvorst, Z.; van der Heyden, F. H. J.; Koopmans, W. J. A.; Gabel, A.; Dekker, C. *Nano Lett.* **2010**, *10*, 765−772.
(11) Firnkes, M.; Pedone, D.; Knezevic, J.; Doblinger, M.; Rant, U. *Nano Lett.* **2010**, *10*, 2162−2167.
(12) Hsu, J. P.; Kao, C. Y. *J. Phys. Chem. B* **2002**, *106*, 10605−10609.
(13) Zhang, M. K.; Ai, Y.; Sharma, A.; Joo, S. W.; Kim, D. S.; Qian, S. Z. *Electrophoresis* **2011**, *32*, 1864−1874.
(14) Qian, S. Z.; Wang, A. H.; Afonien, J. K. *J. Colloid Interface Sci.* **2006**, *303*, 579−592.
(15) Ai, Y.; Qian, S. Z.; Liu, S.; Joo, S. W. *Biomicrofluidics* **2010**, *4*, 013201.
(16) Zhang, M. K.; Yeh, L. H.; Qian, S. Z.; Hsu, J. P.; Joo, S. W. *J. Phys. Chem. C* **2012**, *116*, 4793−4801.
(17) Yeh, L. H.; Zhang, M. K.; Qian, S. Z.; Hsu, J. P. *Nanoscale* **2012**, *4*, 2685−2693.
(18) Ohshima, H. *Colloid Polym. Sci.* **2007**, *285*, 1411−1421.
(19) Wong, J. E.; Diez-Pascual, A. M.; Richtering, W. *Macromolecules* **2009**, *42*, 1229−1238.
(20) Ohshima, H. *J. Colloid Interface Sci.* **2002**, *252*, 119−125.
(21) Zhang, M. K.; Ai, Y.; Kim, D. S.; Jeong, J. H.; Joo, S. W.; Qian, S. Z. *Colloid Surf. B: Biointerfaces* **2011**, *88*, 165−174.
(22) Hill, R. J.; Saville, D. A.; Russel, W. B. *J. Colloid Interface Sci.* **2003**, *258*, 56−74.
(23) Allison, S. *J. Colloid Interface Sci.* **2004**, *277*, 248−254.
(24) Yeh, L. H.; Hsu, J. P. *Soft Matter* **2011**, *7*, 396−411.
(25) Yeh, L. H.; Fang, K. Y.; Hsu, J. P.; Tseng, S. *Colloid Surf. B: Biointerfaces* **2011**, *88*, 559−567.
(26) Hsu, J. P.; Ku, M. H.; Kao, C. Y. *J. Colloid Interface Sci.* **2004**, *276*, 248−254.
(27) Ohshima, H. *Electrophoresis* **2006**, *27*, 526−533.
(28) Duval, J. F. L.; Ohshima, H. *Langmuir* **2006**, *22*, 3533−3546.

(29) Boroudjerdi, H.; Kim, Y. W.; Naji, A.; Netz, R. R.; Schlagberger, X.; Serr, A. *Phys. Rep.-Rev. Sec. Phys. Lett.* **2005**, *416*, 129−199.
(30) Lucy, C. A.; MacDonald, A. M.; Gulcev, M. D. *J. Chromatogr. A* **2008**, *1184*, 81−105.
(31) Wang, L. J.; Keh, H. J. *Microfluid. Nanofluid.* **2011**, *10*, 81−95.
(32) Ye, C. Z.; Sinton, D.; Erickson, D.; Li, D. Q. *Langmuir* **2002**, *18*, 9095−9101.
(33) Ohshima, H. *J. Colloid Interface Sci.* **2003**, *258*, 252−258.
(34) Yeh, L. H.; Hsu, J. P.; Tseng, S. *J. Phys. Chem. C* **2010**, *114*, 16576−16587.
(35) Ren, L. Q.; Li, D. Q. *J. Colloid Interface Sci.* **2001**, *243*, 255−261.
(36) Liu, H.; Bau, H. H.; Hu, H. H. *Langmuir* **2004**, *20*, 2628−2639.
(37) Ai, Y.; Liu, J.; Zhang, B. K.; Qian, S. *Anal. Chem.* **2010**, *82*, 8217−8225.
(38) Allison, S.; Wall, S.; Rasmusson, M. *J. Colloid Interface Sci.* **2003**, *263*, 84−98.
(39) Keh, H. J.; Liu, C. P. *J. Phys. Chem. C* **2010**, *114*, 22044−22054.
(40) Ye, C. Z.; Xuan, X. C.; Li, D. Q. *Microfluid. Nanofluid.* **2005**, *1*, 23−241.
(41) Hsu, J. P.; Yeh, L. H.; Ku, M. H. *Colloid Polym. Sci.* **2006**, *284*, 886−892.
(42) Huang, C. H.; Cheng, W. L.; He, Y. Y.; Lee, E. *J. Phys. Chem. B* **2010**, *114*, 10114−10125.
(43) Hsu, J. P.; Tai, Y. H.; Yeh, L. H.; Tseng, S. *J. Phys. Chem. B* **2011**, *115*, 3972−3980.
(44) Huang, C. H.; Lee, E. *J. Phys. Chem. C* **2012**, *116*, 15058−15067.
(45) Tseng, S.; Cho, C. H.; Chen, Z. S.; Hsu, J. P. *Langmuir* **2008**, *24*, 2929−2937.
(46) Allison, S. A.; Carbeck, J. D.; Chen, C. Y.; Burkes, F. *J. Phys. Chem. B* **2004**, *108*, 4516−4524.
(47) Zhang, X. G.; Hsu, J. P.; Chen, Z. S.; Yeh, L. H.; Ku, M. H.; Tseng, S. *J. Phys. Chem. B* **2010**, *114*, 1621−1631.
(48) O'brien, R. W.; White, L. R. *J. Chem. Soc., Faraday Trans. II* **1978**, *74*, 1607−1626.
(49) Ohshima, H. *Adv. Colloid Interface Sci.* **1995**, *62*, 189−235.
(50) Duval, J. F. L.; Busscher, H. J.; van de Belt-Gritter, B.; van der Mei, H. C.; Norde, W. *Langmuir* **2005**, *21*, 11268−11282.
(51) Duval, J. F. L.; Gaboriaud, F. *Curr. Opin. Colloid Interface Sci.* **2010**, *15*, 184−195.
(52) Yeh, L. H.; Zhang, M.; Hu, N.; Joo, S. W.; Qian, S.; Hsu, J. P. *Nanoscale* **2012**, *4*, 5169−5177.
(53) Hsu, J. P.; Huang, H. T.; Yeh, L. H. *Langmuir* **2012**, *28*, 2997−3004.
(54) Oukacine, F.; Morel, A.; Cottet, H. *Langmuir* **2011**, *27*, 4040−4047.
(55) Keyser, U. F.; van Dorp, S.; Lemay, S. G. *Chem. Soc. Rev.* **2010**, *39*, 939−947.
(56) Fologea, D.; Uplinger, J.; Thomas, B.; McNabb, D. S.; Li, J. L. *Nano Lett.* **2005**, *5*, 1734−1737.
(57) Yeh, L. H.; Liu, K. L.; Hsu, J. P. *J. Phys. Chem. C* **2012**, *116*, 367−373.
(58) Ohshima, H. *Colloid Surf. A: Physicochem. Eng. Aspects* **1995**, *103*, 249−255.
(59) Yeh, L. H.; Hsu, J. P.; Qian, S.; Tseng, S. J. *Electrochem. Commun.* **2012**, *19*, 97−100.
(60) Pevarnik, M.; Healy, K.; Toimil-Molares, M. E.; Morrison, A.; Letant, S. E.; Siwy, Z. S. *ACS Nano* **2012**, *6*, 7295−7302.
(61) Manning, G. S. *J. Phys. Chem.* **1981**, *85*, 1506−1515.
(62) Hoagland, D. A.; Arvanitidou, E.; Welch, C. *Macromolecules* **1999**, *32*, 6180−6190.